ARL-TR-7901 ● Dec 2016

US Army Research Laboratory

Hydrostatic Compression of 2,4,6,8,10,12-hexanitrohexaaza-isowurtzitane (CL20) Co-Crystals

by DeCarlos Taylor and Steve Hunter

NOTICES

Disclaimers

The findings in this report are not to be construed as an official Department of the Army position unless so designated by other authorized documents.

Citation of manufacturer's or trade names does not constitute an official endorsement or approval of the use thereof.

Destroy this report when it is no longer needed. Do not return it to the originator.

ARL-TR-7901 ● DEC 2016

US Army Research Laboratory

Hydrostatic Compression of 2,4,6,8,10,12-hexanitrohexaaza-isowurtzitane (CL20) Co-Crystals

by DeCarlos Taylor
Weapons and Materials Research Directorate, ARL

Steve Hunter
The University of Edinburgh, Edinburgh, Scotland

REPORT DOCUMENTATION PAGE

Form Approved
OMB No. 0704-0188

1. REPORT DATE *(DD-MM-YYYY)*	2. REPORT TYPE	3. DATES COVERED (From - To)
December 2016	Technical Report	October 2015–September 2016

4. TITLE AND SUBTITLE
Hydrostatic Compression of 2,4,6,8,10,12-hexanitrohexaaza-isowurtzitane (CL20) Co-Crystals

5a. CONTRACT NUMBER

5b. GRANT NUMBER

5c. PROGRAM ELEMENT NUMBER

6. AUTHOR(S)
DeCarlos Taylor and Steve Hunter

5d. PROJECT NUMBER

5e. TASK NUMBER

5f. WORK UNIT NUMBER

7. PERFORMING ORGANIZATION NAME(S) AND ADDRESS(ES)
US Army Research Laboratory
ATTN: RDRL-WML-B
Aberdeen Proving Ground, MD 21005-5069

8. PERFORMING ORGANIZATION REPORT NUMBER
ARL-TR-7901

9. SPONSORING/MONITORING AGENCY NAME(S) AND ADDRESS(ES)

10. SPONSOR/MONITOR'S ACRONYM(S)

11. SPONSOR/MONITOR'S REPORT NUMBER(S)

12. DISTRIBUTION/AVAILABILITY STATEMENT
Approved for public release; distribution is unlimited.

13. SUPPLEMENTARY NOTES

14. ABSTRACT

The pressure response of co-crystals of 2,4,6,8,10,12-hexanitrohexaaza-isowurtzitane (CL20) has been determined using quantum molecular dynamics simulations. Co-crystals of CL20 with guest molecules including 2,4,6-trinitrotoluene (TNT), 1,3-dinitrobenzene (DNB), benzotrifuroxan (BTF), and 1,3,5,7-tetranitro-1,3,5,7-tetrazacyclooctane (HMX) were studied and for each system the high pressure (to 50 GPa) unit cell parameters, bulk modulus, and estimates of the shock, particle, and sound velocities are provided.

15. SUBJECT TERMS
Molecular dynamics, co-crystal, energetic materials, compression,CL20, HMX, BTF, DNB

16. SECURITY CLASSIFICATION OF:			17. LIMITATION OF ABSTRACT	18. NUMBER OF PAGES	19a. NAME OF RESPONSIBLE PERSON
a. REPORT	b. ABSTRACT	c. THIS PAGE			DeCarlos Taylor
Unclassified	Unclassified	Unclassified	UU	22	19b. TELEPHONE NUMBER (Include area code) 410-306-0853

Contents

List of Figures

List of Tables

Acknowledgments

All computations were performed at the US Air Force Research Laboratory Department of Defense Supercomputing Resource Center. The project was executed under a cooperative agreement between the US Army Research Laboratory and the University of Edinburgh, Contract No. W911NF-15-2-0095.

INTENTIONALLY LEFT BLANK

1. Introduction

Although the development of new energetic materials (EMs) with decreased sensitivity to initiation and enhanced explosive power is of paramount importance to the Army, the discovery of new EMs that exceed federally mandated standards for safety and stability has proven difficult. Historically, the search for new EMs has focused on synthesis of compounds that share a common chemistry and/or structural motif with existing explosives. However, a novel synthetic approach based on the crystal engineering strategy known as "co-crystallization" has recently been demonstrated as a promising route toward development of new classes of EMs with improved properties.[1,2] Co-crystals are solid state materials comprising 2 (or more) molecular components that interact via noncovalent interactions to form an extended network. As a result of the intermolecular interactions, the co-crystals often have properties that differ from those of the individual components, and this feature has been exploited, with great success, in the medicinal community to enhance the solubility, stability, and bioavailability of active pharmaceutical ingredients.[3] Given the positive impact of co-crystallization on the material properties of pharmaceuticals, co-crystals of a wide variety of EMs such as 2,4,6,8,10,12-hexanitrohexaaza-isowurtzitane (CL20) with the following compounds have now been synthesized:

- 2,4,6-trinitrotoluene (TNT)[1]
- 1,3-dinitrobenzene (DNB)[4]
- Benzotrifuroxan (BTF)[5]
- 1,3,5,7-tetranitro-1,3,5,7-tetrazacyclooctane (HMX)[6]

To date, much of the experimental co-crystal research has focused on synthesis of new compounds using different combinations of EMs. Although a large number of EM co-crystals have been realized, there is a dearth of literature detailing their material properties with most experimental studies to date focused on synthesis and co-crystal structure. There have also been experimental analyses of co-crystal sensitivity to impact and the relation of the co-crystal's stability to that of the individual components.[6,7]

However, other critical material properties such as the response of EM co-crystals to increasing temperature, or mechanical deformation, have not been determined experimentally, and only a limited number of theoretical studies have been reported. Liu et al. used density functional theory (DFT) to perform a hydrostatic compression study (0–100 GPa) of the CL20–HMX co-crystal with analyses of the unit cell volume, band structure, elastic coefficients, and optical absorption

properties.[8] Zhou et al. studied the intermolecular interactions of a series of CL20 co-crystals using the Atoms in Molecules approach and established relations between the strength of intermolecular interactions and the observed sensitivity of the co-crystals.[9] Sun et al.[10] used the COMPASS[11] force field to simulate the structure, energetic, and mechanical properties of CL20–HMX and found that the predicted bulk modulus of the co-crystal was smaller than that of the pure components.

Although the aforementioned hydrostatic compression study of Liu et al. was based on first principles DFT, it was done using static geometry optimization algorithms, which correspond to zero temperature. It is well known that thermal effects, particularly in molecular crystals, can often be pronounced. As an example, the experimentally observed α→γ phase transition in cyclotrimethylene trinitramine (RDX) does not occur when using quantum mechanical (QM) potentials at 0 K.[12] However, inclusion of thermal effects via finite temperature quantum molecular dynamics (QMD) simulation does indeed yield the phase transition at a pressure in excellent agreement with the experiment.[13] Whereas the aforementioned study of Sun et al.[10] did rely upon finite temperature molecular dynamics techniques, the interatomic forces used to propagate the atomic degrees of freedom were obtained using the COMPASS force field.[11] COMPASS is an empirical model, therefore it may not be descriptive of high temperature and pressure structural transformations that may occur in these novel systems. Further, as COMPASS is a nonreactive potential, it has no capability to model thermal or mechanically induced molecular decompositions, which are obviously of paramount importance for explosive energy release.

In this work, we report results of hydrostatic compression of 4 CL20-based co-crystals including CL20–DNB,[4] CL20–BTF,[5] CL20–HMX,[6] and CL20–TNT[1] using QMD simulation. We also include results for the epsilon phase (thermodynamically stable at standard temperature and pressure) of CL20 for comparison.[14] For each crystal we provide the ambient and high-pressure unit cell parameters, the bulk modulus (and its pressure derivative), and shock, particle, and sound velocity data. To our knowledge, the high-pressure data provided in this report (with the exception of ε-CL20[15]) are not currently available experimentally.

2. Computational Methods

The unit cell geometry (Fig. 1) of ε-CL20[14] and all co-crystals[1,4–6] were taken from experiment and the pressure versus volume (PV) isotherms, at a temperature of 300 K, for hydrostatic pressures up to 50 GPa were obtained using QMD simulations. The QMD trajectories (after an initial geometry optimization) were

integrated using the JARVIS[16] software package, which employs a leapfrog algorithm[17] for the atomic coordinates with external pressure imposed via a Berendsen[18] barostat. At each time step, the QM energy and forces were evaluated with the CP2K[19] software package (executed via an external call from JARVIS) using the revised Perdew–Burke–Ernzerhof[20] density functional in a triple zeta valence plus polarization Gaussian basis and the D3 dispersion correction of Grimme et al.[21] The D3 correction was chosen based on its level of agreement with benchmark interaction energies for gas-phase dimers of several energetic molecules including 1,1-diamino-2,2-dinitroethylene (FOX-7), nitrobenzene, and ethylenedinitramine, obtained using coupled cluster theory.[22] Each simulation was run for 5 ps (using a 0.5-fs time step) with time averaged quantities accumulated over the final picosecond of the simulation for all pressures.

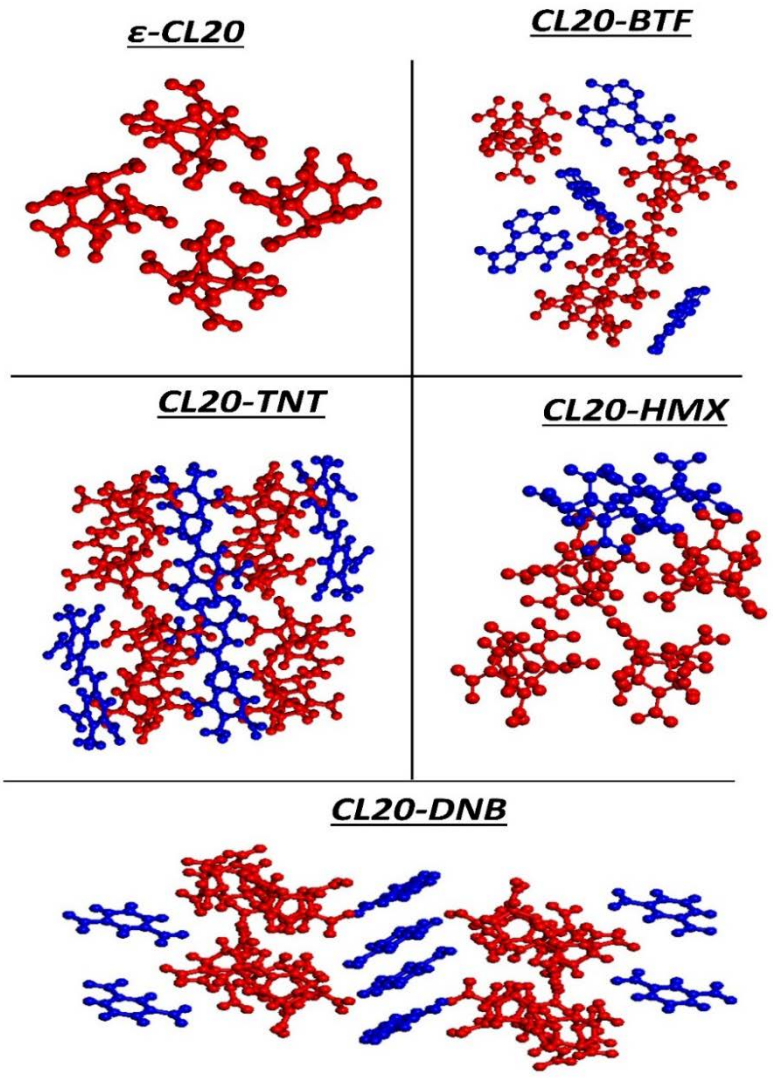

Fig. 1 Experimental unit cell structures of ε-CL20 and co-crystals. For each structure, the CL20 molecules are red and the guest molecules are blue.

3. Results

3.1 PV Data

The predicted unit cell structures at zero pressure and 300 K are compared with the corresponding experimental values in Table 1. The agreement between the computed and experimental data for all systems is good with a maximum deviation of 1.8% for the volume of the CL20–DNB co-crystal. The computed unit cell geometry as a function of pressure is reported in Tables 2 and 3 and the data indicate an anisotropic pressure response for each system. As an example, for the CL20–HMX co-crystal, the *a* and *c* cell vectors show essentially equivalent degrees of compression up to 50 GPa (–13.5%) whereas the *b* vector reduces by almost 20%. Interestingly, our data for CL20–HMX differ from the theoretical predictions of Liu et al.[8] where it was reported that the CL20–HMX co-crystal is "much stiffer" along *a* than the other directions. (As an aside, it should be noted that the *b* and *c* axes are either incorrectly labeled in Fig. 2 of Liu et al.[8] or the DFT results obtained in that study are grossly incorrect.) The different observations between Liu et al.[8] and the present study could be attributable to thermal effects, which were included in the present work whereas the results of Liu et al.[8] correspond to zero temperature.

Table 1 Zero-pressure unit cell structure for ε-CL20 and co-crystals. For each entry, the first number is the simulated value (300 K), the second number is the experimental value,[a] and the third number is the percent difference between simulation and experiment. Lengths in angstroms, angles in degrees, volume in cubic angstroms.

System	*a*	*b*	*c*	α	β	Γ	Volume
ε-CL20	8.807	12.474	13.323	89.99	105.36	90.01	1411.386
	8.791	12.481	13.285	90.00	106.55	90.00	1397.290
	0.18	–0.06	0.29	–0.01	–1.12	0.01	1.01
CL20–BTF	9.226	11.783	21.907	90.00	90.04	89.91	2381.539
	9.275	11.946	21.577	90.00	90.00	90.00	2390.713
	–0.53	–1.36	1.53	0.00	0.04	–0.10	–0.38
CL20–DNB	9.555	13.258	33.230	90.00	89.94	90.01	4209.337
	9.470	13.459	33.620	90.00	90.00	90.00	4285.199
	0.89	–1.49	–1.16	0.00	–0.06	0.01	–1.77
CL20–HMX	16.289	9.854	12.344	89.99	99.21	90.02	1955.885
	16.346	9.936	12.142	90.00	99.23	90.00	1946.530
	–0.35	–0.83	1.66	–0.01	–0.02	0.02	0.48
CL20–TNT	9.719	19.320	24.736	90.00	90.01	90.01	4644.368
	9.674	19.369	24.690	90.00	90.00	90.00	4626.221
	0.46	–0.25	0.19	0.00	0.01	0.02	0.39

[a] Experimental temperatures: ε-CL20/100K, CL20–BTF/293K, CL20–DNB/293K,CL20–HMX/95K, CL20–TNT/95K

Table 2 Unit cell geometry (300 K) as a function of pressure for ε-CL20, CL20–BTF, and CL20–DNB. CL20–BTF simulations were not convergent at 50 GPa.

Pressure	*a*	*b*	*c*	α	β	γ	Volume
ε-CL20							
0.5	8.746	12.338	13.209	89.98	105.26	90.01	1375.141
1	8.697	12.226	13.112	89.97	105.11	90.01	1346.023
1.5	8.651	12.128	13.028	89.95	104.94	90.01	1320.622
2	8.620	12.001	12.956	89.99	104.68	90.03	1296.450
5	8.471	11.621	12.604	89.99	103.91	90.03	1204.361
10	8.291	11.289	12.255	90.01	103.41	90.02	1115.847
20	8.110	10.878	11.800	90.02	103.14	89.98	1013.662
30	7.963	10.647	11.502	90.00	102.90	90.00	950.475
40	7.854	10.468	11.273	90.00	102.73	89.98	903.978
50	7.758	10.336	11.074	90.00	102.54	89.99	866.761
CL20–BTF							
0.5	9.125	11.660	21.770	89.98	90.06	89.93	2316.269
1	9.005	11.568	21.675	90.02	90.01	89.96	2257.862
1.5	8.932	11.483	21.582	90.00	90.05	90.03	2213.621
2	8.866	11.408	21.518	90.03	90.04	89.93	2176.445
5	8.607	11.096	21.111	89.99	90.01	89.94	2016.183
10	7.883	11.031	21.115	90.25	88.69	88.84	1835.101
20	7.542	10.672	20.589	90.42	88.65	88.74	1656.175
30	7.272	10.474	20.291	90.43	88.85	88.79	1544.905
40	6.797	10.590	20.174	89.32	90.18	91.81	1451.257
50	. . .	. . .	. . .	. . .	. . .	. . .	. . .
CL20–DNB							
0.5	9.425	13.169	32.958	90.01	89.99	90.00	4090.529
1	9.327	13.127	32.701	89.99	89.97	90.01	4003.731
1.5	9.247	13.099	32.433	90.00	90.03	90.00	3928.662
2	9.188	13.061	32.198	90.02	90.00	89.98	3863.821
5	8.929	12.857	31.147	90.02	89.99	90.01	3575.463
10	8.690	12.595	30.143	90.00	90.00	89.99	3299.152
20	8.379	12.205	29.030	89.99	90.00	90.04	2968.959
30	8.186	11.918	28.399	89.96	89.98	89.97	2770.411
40	8.036	11.727	27.865	90.09	89.94	90.04	2626.031
50	7.898	11.563	27.535	89.98	90.28	89.95	2514.604

Table 3 Unit cell geometry (300 K) as a function of pressure for CL20–HMX and CL20–TNT. CL20–TNT simulations were not convergent at 50 GPa.

Pressure	a	b	c	α	β	γ	Volume
CL20–HMX							
0.5	16.177	9.763	12.226	89.97	99.10	90.00	1906.628
1	16.096	9.695	12.133	90.01	99.08	89.98	1869.646
1.5	15.989	9.631	12.076	90.02	98.93	90.00	1837.104
2	15.946	9.588	11.966	90.04	99.08	90.01	1806.603
5	15.645	9.285	11.725	90.05	99.00	89.98	1682.302
10	15.305	8.959	11.512	90.01	98.86	90.04	1559.678
20	15.190	7.891	11.758	89.97	98.07	90.12	1395.449
30	14.841	7.710	11.510	89.87	97.73	90.34	1305.060
40	14.595	7.594	11.277	89.75	97.51	90.50	1239.080
50	14.079	7.932	10.690	90.45	95.40	89.84	1188.418
CL20–TNT							
0.5	9.649	19.084	24.567	90.00	89.98	90.02	4523.402
1	9.600	18.822	24.448	90.00	89.97	90.00	4417.430
1.5	9.547	18.659	24.326	89.99	89.99	89.99	4333.494
2	9.481	18.517	24.249	89.98	89.98	89.99	4257.111
5	9.274	17.902	23.749	89.99	90.01	90.00	3942.715
10	8.973	17.265	23.411	90.00	90.04	90.00	3626.657
20	8.619	16.480	22.988	89.98	89.99	89.99	3265.369
30	8.395	16.009	22.634	90.00	90.00	90.01	3041.775
40	8.242	15.656	22.316	89.98	89.99	90.05	2879.749
50	. . .	. . .	. . .	. . .	. . .	. . .	. . .

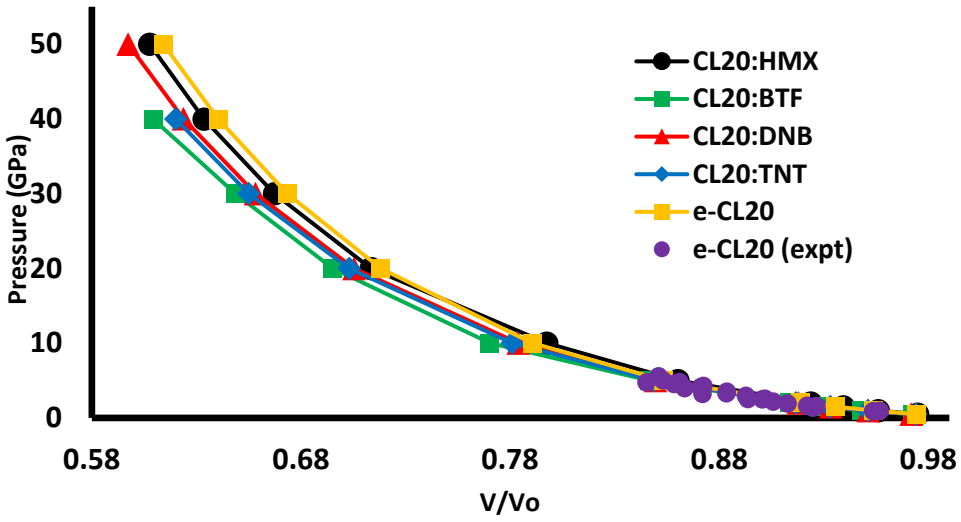

Fig. 2 PV data for ε-CL20 and co-crystals. Experimental data taken from Gump et al.[15]

Plots of the computed unit-cell volume as a function of pressure are presented in Fig. 2. As shown, the pressure response of the co-crystals is very similar to that of ε-CL20 and only show a slight reduction in stiffness at high pressure. At this time, we cannot conclusively comment on the presence of pressure-induced phase transitions in the co-crystals. The current data show no evidence of high-pressure phase transitions, but longer time simulations with larger computational cells may show different behavior. This will be the subject of a future study using linear scaling QM techniques[23] with first principles DFT or using semi-empirical Hamiltonians such as tight-binding[24] to simulate larger cells for longer periods.

3.2 Derived Data

The bulk modulus and approximations to the Hugoniot shock and particle velocity values were obtained using the isothermal PV data. Table 4 contains the bulk modulus (K), and pressure derivative (K'), of each co-crystal.

Table 4 Bulk modulus (K) and pressure derivative (K') of CL20 co-crystals

Crystal	K(GPa)	K'
CL20–BTF	15.27	8.45
CL20–DNB	15.78	9.54
CL20–HMX	18.53	8.02
CL20–TNT	16.98	6.97
ε-CL20	17.81	7.46
ε-CL20(expt)[a]	16.88	3.82

[a] Experimental data limited to points below 2 GPa for comparison.

The moduli were determined by fitting all pressure points (up to 2 GPa) to the third order Birch–Murnaghan[25] equation of state. With the exception of the CL20–HMX co-crystal, all systems show a reduction in the value of the bulk modulus relative to the ε-CL20 reference. The predicted value of 18.53 GPa for the CL20–HMX co-crystal is to be compared with the reported value of 8.3 GPa reported in Sun et al.[10]. The value in Sun et al.[10] was obtained using the COMPASS force field whereas the result reported in the present work was obtained using an ab initio potential. Although one would generally consider an ab initio potential to be more accurate, our values may be suffering from size effects, which can lead to materials that are too stiff under load. Thus, our predicted values may be too large. An experiment will be necessary to resolve the differences between this work and the previous study.

Table 5 contains the predicted sound speed, shock (U_s), and particle (U_p) velocities that were obtained from the PV data using the standard relations.[26] These values represent approximations to the true Hugoniot loci since the PV data in this study

correspond to 300 K, and the associated temperature increase that would result from shock compression was not incorporated. With that caveat, a plot of the corresponding shock and particle velocities is given in Fig. 3 and, as shown, all curves are essentially linear. However, as stated previously, using the current simulation length and time scales, we cannot at this time conclusively exclude the existence of phase transitions which would appear as discontinuities in the Us-Up curves in Fig. 3.

Table 5 Predicted sound, shock, and particle velocity values of co-crystals. All values obtained using isothermal compression data from QMD simulation at 300 K. All velocities in km/s.

	CL20–BTF		CL20–DNB		CL20–HMX		CL20–TNT	
Pressure	**Us**	**Up**	**Us**	**Up**	**Us**	**Up**	**Us**	**Up**
0.5	0.08	3.07	0.09	3.04	0.08	3.16	0.08	3.18
1	0.16	3.16	0.16	3.27	0.15	3.38	0.16	3.28
1.50	0.23	3.32	0.23	3.43	0.21	3.52	0.23	3.43
2	0.30	3.47	0.29	3.56	0.28	3.62	0.30	3.55
5	0.63	4.12	0.63	4.17	0.59	4.24	0.63	4.17
10	1.09	4.76	1.06	4.92	1.01	4.98	1.07	4.90
20	1.78	5.84	1.76	5.96	1.70	5.92	1.77	5.95
30	2.34	6.66	2.32	6.77	2.24	6.73	2.33	6.76
40	2.85	7.29	2.80	7.46	2.71	7.41	2.83	7.44
50	. . .	. . .	3.24	8.06	3.14	8.00	. . .	. . .
Sound speed	3.00		3.09		3.21		3.10	

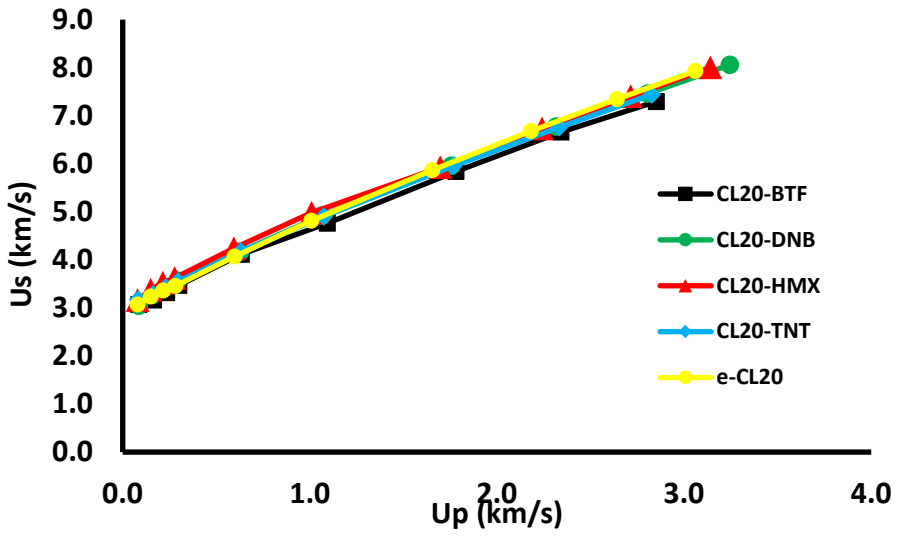

Fig. 3 Predicted shock and particle velocities. Lines have been added as guides to the eye.

4. Conclusion

In the absence of experiment, computational modeling, particularly those methods based on first principles quantum mechanics, can provide material properties that are in very good agreement with measured data. However, a true determination of the accuracy of the current results can only be obtained through experimental validation. Ultimately, we would like to develop predictive methods that would enable a priori evaluation of the performance of a co-crystal based on the properties of the individual components. The data provided in this report can be of value in the establishment of these types of metrics via comparison of the co-crystal data that we have provided to that of the individual components. However, more data for a much wider variety of energetic co-crystals will have to be computed before a general correlation can be established. As stated, the shock and particle velocity data in this work are approximate since they were computed from isothermal compression values. Precise determination of true Hugoniot points using QMD simulation is currently underway, and the initial simulations indicate a significant increase in system temperature with increasing shock pressure. This in turn drives chemical reactivity in several of the co-crystals at modest pressures. A complete Hugoniot study will be the subject of a future report.

5. References

1. Bolton O, Matzger AJ. Angew Chem Int Ed. 2011;50(38):8960.
2. Aakeröy C, Wijethunga T, Desper J. Chem Eur J. 2015;21(31):11029.
3. Schultheiss N, Newman A. Crys Gro Des. 2009;9(6):2950.
4. Wang Y, Yang Z, Li H, Zhou X, Zhang Q, Wang J, Liu Y. Prop Explo Pyro. 2014;39(4):590.
5. Yang Z, Li H, Zhou X, Zhang C, Huang H, Li J, Nie F. Crys Gro Des. 2012;12(11):5155.
6. Bolton O, Simke LR, Pagoria PF, Matzger AJ. Crys Gro Des. 2012;12(9):4311.
7. Landenberger K, Bolton O, Matzger A. J Am Chem Soc. 2015;137(15):5074.
8. Liu Z, Wu Q, Zhu W, Xiao H. Roy. Soc Chem Adv. 2015;5(43):34216.
9. Zhou J, Shi L, Zhang C, Li H, Chen M, Chen W. J Mol Str. 2016;1116:93.
10. Sun T, Xiao J, Liu Q, Zhao F, Xiao H. J Mat Chem A. 2014;2(34):13898.
11. Sun H. J Phys Chem B. 1998;102(38):7338.
12. Taylor D. J Appl Phys. 2014;116(5):053513.
13. Sorescu D, Rice B. J Phys Chem C. 2016;120(35):19547.
14. Bolotina N, Hardie M, Speer R, Pinkerton A. J Appl Crystallogr. 2004;37(5):808.
15. Gump J, Peiris S. J Appl Phys. 2008;104(8):083509.
16. JARVIS is a crystal structure optimization and molecular dynamics software package developed by D Taylor at the Army Research Laboratory (US).
17. Allen M, Tildeslay D. Computer simulation of liquids. Oxford (England): Clarendon Press; 1987.
18. Berendsen H, Postma J, van Gunsteren W, DiNola A, Haak J. J Chem Phys. 1984;81(8):3684.
19. CP2K. Open source molecular dynamics. [accessed 2016 May 1]. https://www.cp2k.org/.
20. Zhang Y, Yang W. Phys Rev Lett. 1998;80(4):890.

21. Grimme S. J Comp Chem. 2004;25(12):1463.

22. Taylor D, Angyan J, Galli G, Zhang C, Gygi F, Hirao K, Won Song J, Rahul K, von Lilienfeld A, Podeszwa R, et al. J Chem Phys. 2016;145(12):124105.

23. VandeVondele J, Borstnik U, Hutter J. J Chem T Comp. 2012;8(10):3565.

24. Elstner M, Porezag D, Jungnickel G, Elsner J, Haugk M, Frauenheim T, Suhai S, Seifert G. Phys Rev B. 1998;58(11):7260.

25. Birch F. Phys Rev. 1947;71(11):809.

26. Cooper P. Explosives engineering. New York (NY): John Wiley and Sons; 1996.

List of Symbols, Abbreviations, and Acronyms

BTF	benzotrifuroxan
CL20	2,4,6,8,10,12-hexanitrohexaaza-isowurtzitane
DFT	density functional theory
DNB	1,3-dinitrobenzene
EM	energetic material
FOX-7	1,1-diamino-2,2-dinitroethylene
HMX	1,3,3,7-tetranitro-1,3,5,7-tetrazacyclooctane
PV	pressure versus volume
QM	quantum mechanical
QMD	quantum molecular dynamics
RDX	cyclotrimethylene trinitramine
TNT	2,4,6-trinitrotoluene

1 (PDF) DEFENSE TECHNICAL INFORMATION CTR DTIC OCA

2 (PDF) DIRECTOR US ARMY RESEARCH LAB RDRL CIO L IMAL HRA MAIL & RECORDS MGMT

1 (PDF) GOVT PRINTG OFC A MALHOTRA

24 (PDF) DIR USARL
RDRL WM
B FORCH
J ZABINSKI
RDRL WML
W OBERLE
M ZOLTOSKI
RDRL WML B
N TRIVEDI
J MORRIS
B RICE
E BYRD
W MATTSON
J CIEZAK-JENKINS
T JENKINS
F DELUCIA
J GOTTFRIED
R PESCE-RODRIGUEZ
S WEINGARTEN
I BATYREV
B BARNES
R SAUSA
RDRL WML C
S AUBERT
J SABATINI
J BANNING
RDRL WML D
R BEYER
J VEALS
M MCQUAID

INTENTIONALLY LEFT BLANK.